

Influence of Elemental Iodine on Imidazolium-Based Ionic Liquids: Solution and Solid-State Effects

Zhaofu Fei, Félix D. Bobbink, Emilia Păunescu, Rosario Scopelliti, and Paul J. Dyson*

Institut des Sciences et Ingénierie Chimiques, Ecole Polytechnique Fédérale de Lausanne (EPFL), CH-1015 Lausanne, Switzerland

S Supporting Information

ABSTRACT: Ionic liquids doped with I_2 , usually resulting in the formation of polyiodide anions, are extensively used as electrolytes and in iodination reactions. Herein, NMR spectroscopy and single-crystal X-ray diffraction were used to rationalize the structures of imidazolium-based polyiodide ionic liquids in the liquid and solid states. Combined, these studies show that extensive interactions between the imidazolium cation and the resulting polyiodide anion are present, which have the net effect of lengthening, polarizing, and weakening the I–I bonds in the anion. This bond weakening rationalizes the high conductivity and reactivity of ionic liquids doped with I_2 .



INTRODUCTION

Polyiodide salts comprise a structurally diverse series of materials,^{1,2} in which $[I_3]^-$ is the simplest and most common congener. The intrinsic weakness of the I–I bond (in elemental iodine the bond dissociation energy is 36 kcal/mol) leads to the facile dissociation of polyiodide species into smaller fragments, that is, I^- and I_2 , and, in this respect, polyiodides may be considered as adducts of I^- with various ratios of I_2 . Many different polyiodides of general formula $[I_{2n+1}]^-$ have been reported, and to the best of our knowledge $[I_{29}]^-$ is the largest polyiodide characterized to date.^{3,4}

In the solid state, polyiodides are stabilized by a wide range of structurally diverse counter-cations including metal-based,^{4,5} ammonium, phosphonium,^{6,7} bipyridinium,⁸ and sulfonium cations.⁹ However, the properties of polyiodides in the solid state have not been systematically studied, despite polyiodides in the liquid/solution states exhibiting interesting properties leading to their application in electronic devices,¹⁰ batteries,^{11,12} optical devices,^{13,14} and dye-sensitized solar cells.^{15,16}

In addition, ionic liquid–polyiodide systems have been applied as iodination reagents/solvents in organic synthesis,^{17–20} with the reaction rate dependent on the nature of the ionic liquid anion.²¹ Iodide-containing ionic liquids have also been used to remove and store radioactive iodine with interactions between iodide and the iodine believed to contribute to the efficiency of the ionic liquid used in this application.²² Imidazolium iodide ionic liquids with added I_2 , notably mixtures of 1-propyl-3-methylimidazolium iodide, [pmim] I , with I_2 , have been frequently used as redox pairs in dye-sensitized solar cells,^{16,17} and it was proposed that the Grotthuss mechanism could be responsible for the increased conductivity of the polyiodide species.²⁴ A recent study indicated that the Grotthuss mechanism is a significant contributor to the conductivity of these types of systems and

provided new insights into ion pairing processes and the formation of polyiodide species.^{23,24}

Despite these studies the nature of polyiodides/ I_2 in ionic liquids, with respect to structure and bonding, remains poorly understood. A large number of solid-state structures containing polyiodides with different cations have been reported,² but to the best of our knowledge there is only one example involving an imidazolium cation, namely, a 1:1 adduct of the zwitterion 1,3-bis(carboxymethyl)imidazolium with 1,3-bis(carboxymethyl)imidazolium triiodide.²⁵ Gas-phase studies, however, indicate that many different polyiodides exist, up to $[I_{17}]^-$ in combination with the 1-propyl-3-methylimidazolium cation.²⁶

Herein, we describe an investigation of the effect of I_2 addition to a series of imidazolium salts. The stepwise formation of polyiodides is revealed, and the spectroscopic signatures and solid-state structures of the resulting materials are determined.

RESULTS AND DISCUSSION

The ionic liquids used in this study are shown in Figure 1. Initial spectroscopic studies employed [pmim] I ,^{27,28} the benchmark ionic liquid used as an electrolyte in solvent-free dye-sensitized solar cells with added I_2 to generate the I^-/I_3^- redox pair.^{15,16} The 1H NMR spectrum of [pmim] I in deuterated solvents has been reported previously,^{29,30} but as far as we are aware, NMR spectra of this ionic liquid in pure form, that is, not dissolved in a deuterated molecular solvent, have not been reported. Note that NMR spectroscopy has been extensively used to study ionic liquids;³¹ however, there are

Received: September 1, 2015

Published: October 14, 2015

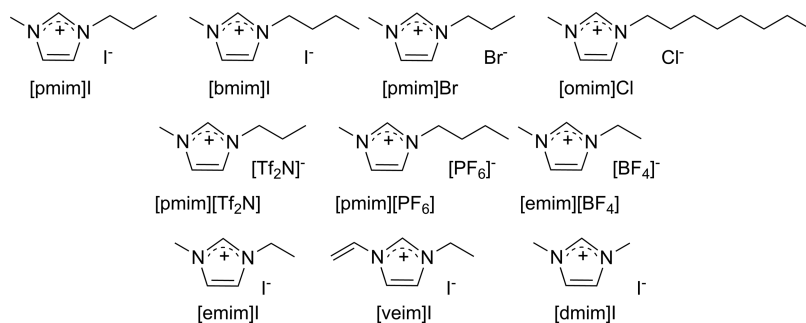


Figure 1. Structures of the ionic liquids employed in the study. $[pmim]^+$ = 1-propyl-3-methyl imidazolium; $[bmim]^+$ = 1-butyl-3-methylimidazolium; $[emim]^+$ = 1-ethyl-3-ethylimidazolium; $[omim]^+$ = 1-octyl-3-methylimidazolium; $[veim]^+$ = 1-vinyl-3-ethylimidazolium; $[dmim]^+$ = 1,3-dimethylimidazolium.

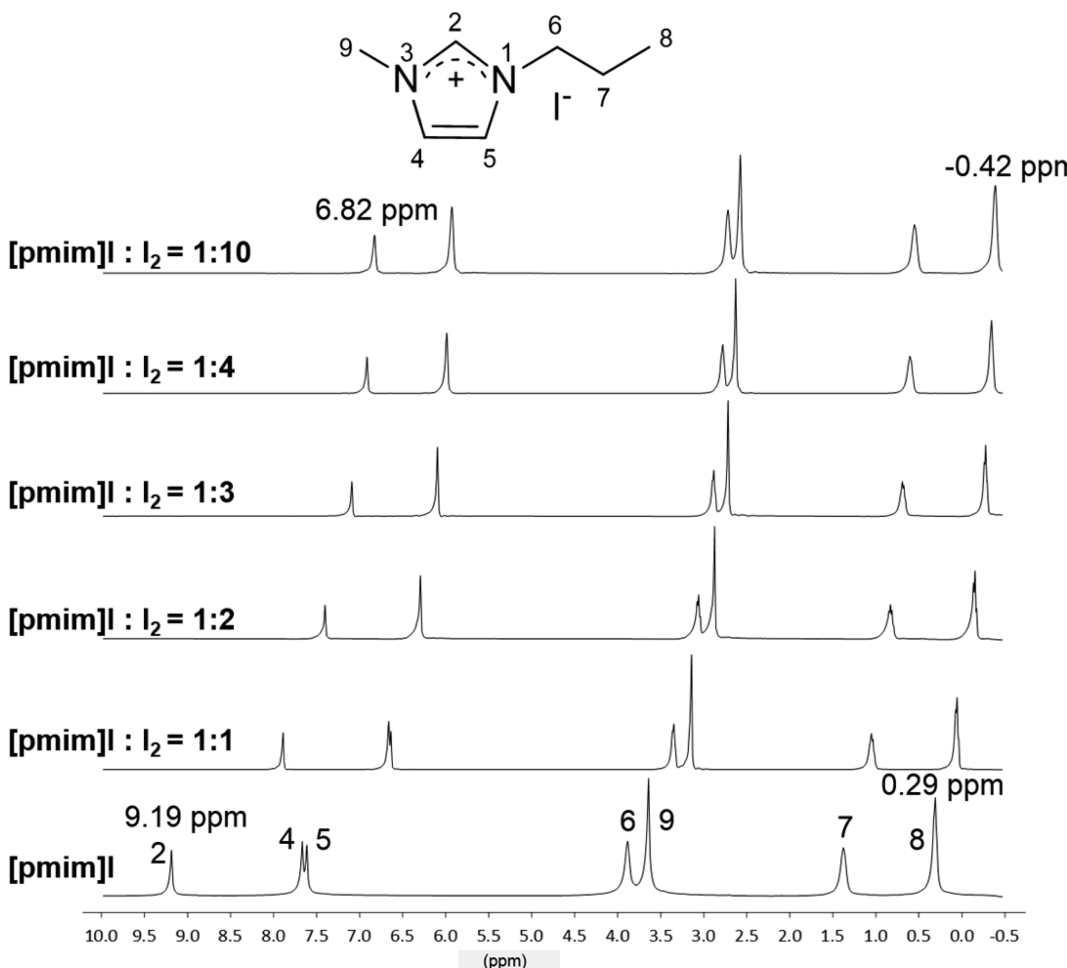


Figure 2. Structure of the $[pmim]^+$ cation with atom numbering scheme and ^1H NMR spectra of $[pmim]\text{I}$ with added I_2 in the range of $-0.5\text{--}10.0$ ppm.

comparatively few NMR studies of neat room-temperature ionic liquids.^{32,33}

The ^1H NMR spectrum of neat $[pmim]\text{I}$ is significantly different than the spectrum of $[pmim]\text{I}$ dissolved in CDCl_3 . For example, in CDCl_3 the signal for terminal aliphatic $-\text{CH}_3$ group in the propyl substituent is observed at ca. 0.89–0.95 ppm,^{34,35} whereas in the neat ionic liquid the same peak is observed at 0.28 ppm.^{29,30} As expected, the addition of elemental I_2 to $[pmim]\text{I}$ alters the ^1H NMR spectrum (Figure 2), presumably since the stepwise addition of I_2 to $[pmim]\text{I}$ affords polyiodide species of formula $[pmim][\text{I}_{2n+1}]$ ($n = 1, 2, 3$,

etc.).^{23,24,26} As the amount of added I_2 increases the peak corresponding to the acidic proton in position 2 of the imidazolium ring changes dramatically, shifting to lower frequency, that is, from 9.19 to 6.82 ppm.

The magnitude of the shielding depends on the molar ratio of $[pmim]\text{I}/\text{I}_2$, which changes rapidly until reaching a ratio of 1:4 (6.94 ppm), after which further addition of elemental iodine results in only small changes to the ^1H NMR spectrum. At a molar ratio of $[pmim]\text{I}/\text{I}_2$ of 1:10 the 2-H signal is observed at 6.82 ppm (elemental iodine crystals are also observed), and the signals corresponding to the protons at positions 4 and 5 of the

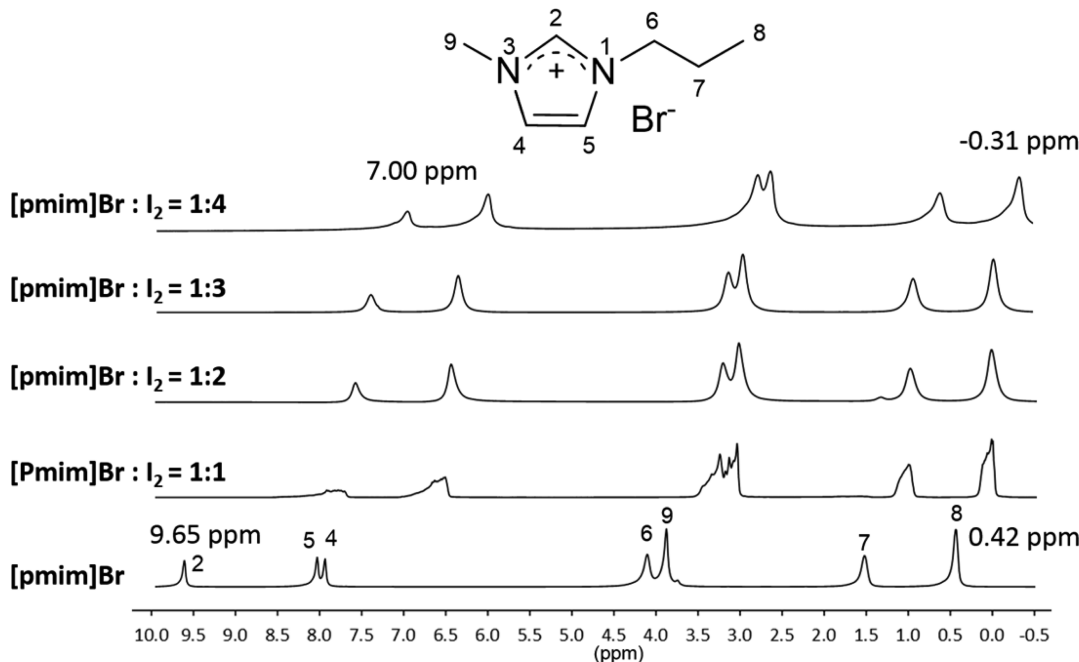


Figure 3. Structure of the $[\text{pmim}]^+$ cation with atom numbering scheme and ^1H NMR spectra of $[\text{pmim}]\text{Br}$ with added I_2 in the range of -0.5 – 10.0 ppm.

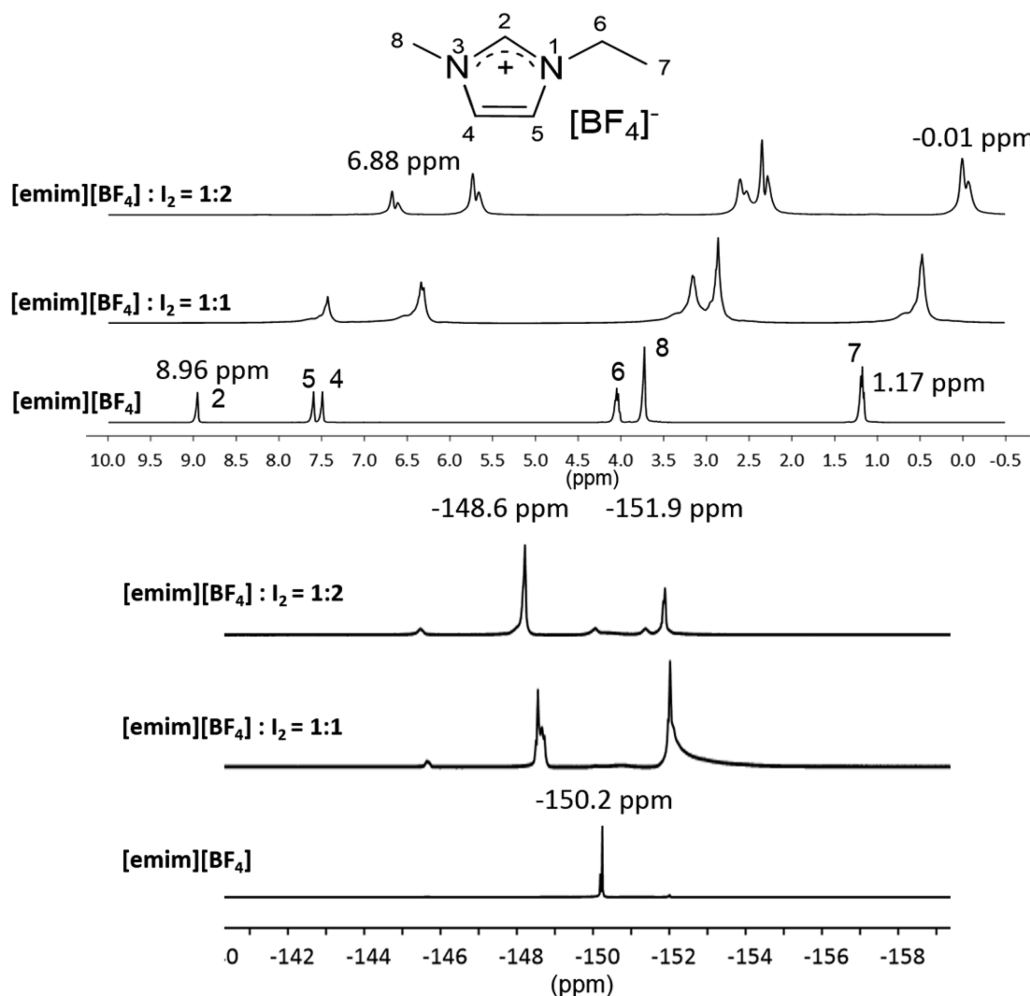


Figure 4. Structure of the $[\text{emim}]^+$ cation with atom numbering scheme and ^1H NMR spectra of $[\text{emim}][\text{BF}_4]$ with added I_2 in the range of -0.5 – 10.0 ppm.

imidazolium cation coalesce. The magnitude of the shielding of the protons in the imidazolium ring is not unexpected and is presumably due to H-bonding interactions between the acidic ring protons, and the polyiodide anion—similar effects have been observed for interactions with solvents^{34–39} and the ionic liquid anion (in neat ionic liquids).^{40,41}

The peaks corresponding to the aliphatic hydrogen atoms in the side chains also move to lower frequencies as the molar ratio of [pmim]I/I₂ increases. In [pmim]I the chemical shift of the –CH₃ group in the propyl chain is observed at 0.29 ppm in the pure liquid and at –0.42 ppm in the ionic liquid saturated with I₂ (Figure 2, top). This change ($\Delta = 1.3$ ppm) is considerably greater than that observed in organic solvents, typically $\Delta < 0.05$ ppm.^{31,32} Changes to the peaks corresponding to the ring C atoms in the ¹³C NMR spectra undergo only minor changes as the [pmim]I/I₂ ratio changes, and the signals corresponding to the aliphatic carbon atoms are not observed to change (Figure S1).

1-Butyl-3-methylimidazolium iodide, [bmim]I, is also liquid at room temperature^{29,42} and was studied similarly to [pmim]I, with similar changes in the ¹H NMR spectra observed. In a saturated solution of elemental iodine in [bmim]I the signals corresponding to the imidazolium ring protons are observed at lower frequencies than those in the pure liquid, $\Delta\delta_H = 2.08$ ppm for the most acidic 2-H.

Analysis of X-ray crystal structures of salts containing polyiodide anions reveals, in many cases, a “channel inclusion feature”; that is, the cations are organized in channels encased in polyiodide (I₃[–], I₅[–], or I₇[–]) layers.⁴³ If such a structure were to persist in the liquid phase it would account for the strong shielding of the protons of the cation in the ¹H NMR spectrum. Indeed, channel inclusion feature-type structures were established in the solid state for some of the ionic liquids studied herein (see below).

1-Propyl-3-methylimidazolium bromide, [pmim]Br, is also liquid at room temperature,⁴⁴ and the stepwise addition of I₂ to this ionic liquid led to similar spectroscopic changes to those described above. In pure [pmim]Br the peak corresponding to 2-H of the imidazolium is observed at 9.65 ppm, and at a molar ratio of [pmim]Br/I₂ of 1:4 the corresponding peak is observed at 7.0 ppm ($\Delta = 2.65$ ppm, which is greater than that observed for [pmim]I/I₂ at about the same molar ratio, $\Delta = 2.25$ ppm). The peak attributable to the –CH₃ group in the propyl chain changes from 0.42 ppm in [pmim]Br to –0.31 ppm in [pmim]Br/I₂, 1:4 ratio (Figure 3).³³

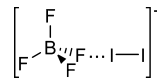
The chloride-based ionic liquid 1-octyl-3-methylimidazolium chloride, [omim]Cl, represents a rare example of an imidazolium chloride that is liquid at room temperature,⁴² albeit a highly viscous wax-like one, but nevertheless is amenable to study by ¹H NMR spectroscopy (Figure S2). Addition of elemental I₂ to [omim]Cl noticeably decreases the viscosity of the solution. In a saturated solution a shift toward lower frequencies of the signals corresponding to the imidazolium ring proton is observed, with $\Delta\delta_H$ for the 2-H proton being ca. 2 ppm.

Elemental I₂ was also added to ionic liquids composed of nonhalide anions, that is, bis(trifluoromethylsulfonyl)imide [Tf₂N][–], hexafluorophosphate [PF₆][–], and tetrafluoroborate [BF₄][–]. I₂ is poorly soluble in [pmim][Tf₂N] and [bmim][PF₆], and the frequencies at which the imidazolium ring protons are observed in the ¹H NMR spectra hardly change (Figures S3 and S4). In contrast, I₂ readily dissolves in 1-ethyl-3-methylimidazolium tetrafluoroborate, [emim][BF₄], up to 2

equivalents of I₂, and large changes were observed in the ¹H NMR spectra for all the protons of the imidazolium cation as the [bmim][BF₄]/I₂ ratio increases (Figure 4). In pure [emim][BF₄] the peak corresponding to 2-proton of the imidazolium is observed at 8.96 ppm, and at a molar ratio of [emim][BF₄]/I₂ of 1:2 the corresponding peak is observed at 6.88 ppm ($\Delta = 2.08$ ppm). The peak attributable to the –CH₃ group in the propyl chain changes from 1.17 ppm in [emim][BF₄] to –0.01 ppm in [emim][BF₄]/I₂, in a 1:2 ratio.

The differences in the solubility of I₂ in [pmim][Tf₂N] and [bmim][PF₆] compared to [emim][BF₄] may be attributed to the differences in charge delocalization in the anion,^{45,46} a key factor that governs the properties of the ionic liquids.^{47,48} The negative charge in [BF₄][–] is less delocalized than in [PF₆][–] and [Tf₂N][–], giving rise to stronger F···I interactions. Similar observations have been reported for BF₃ dissolved in [emim][BF₄].⁴⁹ The [BF₄][–] anion in [emim][BF₄] is able to polarize I₂ via the formation of F···I interactions (Scheme 1), as

Scheme 1. Proposed Interaction of I₂ with the BF₄[–] Anion



indicated from a comparison of the ¹⁹F NMR spectra of pure [emim][BF₄] and [emim][BF₄]/I₂ with a molar ratio of 1:1. The ¹⁹F NMR spectrum of [emim][BF₄] displays a singlet at –150.2 ppm, whereas the spectrum of 1:1 molar ratio of [emim][BF₄]/I₂ contains two signals at –148.6 and –151.9 ppm, with approximately equal intensities (Figure 4), indicative of a strong interaction between the [BF₄][–] anion and iodine (Scheme 1). At a 1:2 molar ratio of [Bmim][BF₄]/I₂ the ¹⁹F NMR spectrum does not change much; the main difference is that the intensity of the signal at –148.6 ppm increases relative to the one at –151.9 ppm.

As mentioned above, ionic liquid–I₂ mixtures are used in iodination reactions,^{17–20} and our findings help to rationalize the high catalytic activity of these systems including the observed anion effects, that is, ionic liquids with anions that have a more localized charge polarize iodine, which activates it and leads to high reactivity in iodination reactions. In addition these anions, [BF₄][–], favor iodine solubility, which is advantageous in the removal of radioactive iodine.²²

Solid-State Studies. Structural features of certain polyiodide systems described herein were ascertained by X-ray diffraction analysis from crystals grown by *in situ* crystallization of the ionic liquid–I₂ mixture at low temperature (see Experimental).⁵⁰ Crystals were obtained with the [emim]⁺ and 1-vinyl-3-ethylimidazolium, [veim]⁺,⁵¹ cations. Addition of I₂ to [emim]I or [veim]I in a 1:1 molar ratio followed by mild heating at 60 °C and slow cooling to room temperature leads to the formation of black crystals of formula [emim][I₃] and [veim][I₃], respectively (Figure 5). Crystals comprising these cations suitable for X-ray diffraction analysis could not be obtained with higher molar ratios of I₂.

Although numerous crystal structures containing polyiodide anions have been reported^{2,52,53} to the best of our knowledge the structures of [emim][I₃] and [veim][I₃] represent the first polyiodides with simple imidazolium cations. A 1:1 adduct of the zwitterion 1,3-bis(carboxymethyl)imidazolium and 1,3-bis(carboxymethyl)imidazolium triiodide is known in which the [I₃][–] anion forms a linear structure (with a 180° I–I–I

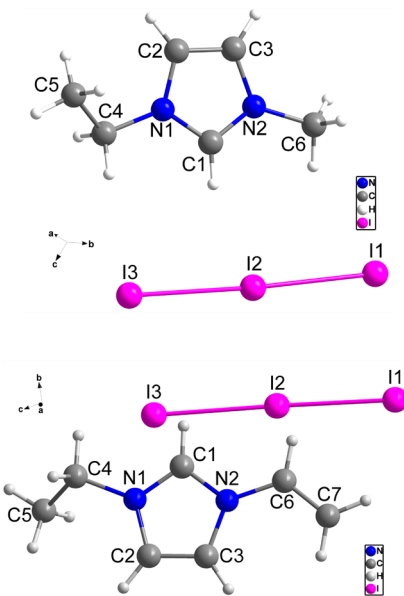


Figure 5. (upper) ORTEP representation of the structure of $[\text{emim}][\text{I}_3]$ (selected bond lengths (\AA) and angles (deg): N(1)–C(1) 1.341(4), N(2)–C(1) 1.328(4), C(2)–C(3) 1.350(4), C(4)–C(5) 1.517(4), I(1)–I(2) 2.9208(3), I(2)–I(3) 2.9501(3), N(2)–C(1)–N(1) 108.6(3), I(1)–I(2)–I(3) 177.195(9). (lower) ORTEP representation of the structure of $[\text{veim}][\text{I}_3]$ (selected bond lengths (\AA) and angles (deg): N(1)–C(1) 1.328(15), N(1)–C(4) 1.499(16), C(2)–C(3) 1.357(18), C(4)–C(5) 1.50(2), C(6)–C(7) 1.331(18), I(1)–I(2) 2.8854(16), I(2)–I(3) 2.9625(16), N(1)–C(1)–N(2) 108.4(10), I(1)–I(2)–I(3) 176.89(3).

angle) and is stabilized by the carboxyl groups (the I–I distance is 2.9192(6) \AA).²⁵ In crystalline polyiodide species the iodide $[\text{I}]^-$, triiodide $[\text{I}_3]^-$, and I_2 represent basic units for the

construction of more complicated oligomeric polyiodide species.² The triiodide anion can be symmetrical or unsymmetrical and linear or bent depending on the nature of the cation.

The bond parameters within the cation in $[\text{emim}][\text{I}_3]$ are similar to those observed in $[\text{emim}]\text{I}$,⁵⁴ although the length of the C2–C3 bond in $[\text{emim}][\text{I}_3]$ is slightly longer than the corresponding bond in $[\text{emim}]\text{I}$ (1.350(4) vs 1.322(7) \AA).⁵⁴ The triiodide anion in $[\text{emim}][\text{I}_3]$ is both unsymmetrical (I_1 – I_2 = 2.9208(3) \AA and I_2 – I_3 = 2.9501(3) \AA , 2.715(1) \AA for I_2)⁵⁵ and slightly bent (I_1 – I_2 – I_3 = 177.195(9) $^\circ$; Figure 5, upper). The structure of the triiodide anion in $[\text{veim}][\text{I}_3]$ is somewhat more distorted than that of $[\text{emim}][\text{I}_3]$ (I_1 – I_2 = 2.885(2), I_2 – I_3 = 2.963(2), I_1 – I_2 – I_3 = 176.89(3) $^\circ$; Figure 5, lower). The I–I bond lengths observed in $[\text{emim}][\text{I}_3]$ and $[\text{veim}][\text{I}_3]$ are typical of those found in other structures containing the $[\text{I}_3]^-$ anion, which in some cases can be as long as 4.2 \AA .^{1,2}

In the crystal of $[\text{emim}][\text{I}_3]$ the triiodide anion form chains through the terminal I_1 and I_3^{iv} atoms with $\text{I}\cdots\text{I}$ distances of 3.96 \AA (Figure 6). All three iodide atoms in the anion are involved in hydrogen bonds with almost all the hydrogen atoms of the cation, corroborating the NMR spectra described above which show all the protons are effected by the polyiodide anions. Of note, the central iodide atom, I_3^{iii} , forms the shortest hydrogen bonds with the hydrogen atoms from the ring (I_3^{iii} –H3 = 3.12 \AA (Figure 6)). The anion also forms weak $\text{I}\cdots\pi$ interactions ($\text{I}_1^{ii}\cdots\pi$ = 3.86 \AA), which presumably contribute to the changes observed in the NMR spectra.

The crystal of $[\text{veim}][\text{I}_3]$ contains a hydrogen bond network similar to the one present in $[\text{emim}][\text{I}_3]$ (Figure 7), with hydrogen bonds between the anion and the imidazolium ring protons ranging from 3.03 (I_2^{ii} –H1) to 3.08 \AA (I_2^{iv} –H3), and those with the hydrogen atoms in the side chain ranging from 3.22 \AA (I_1^{iii} –HSC) to 3.24 \AA (I_1^{ii} –H4B). In the $[\text{veim}][\text{I}_3]$

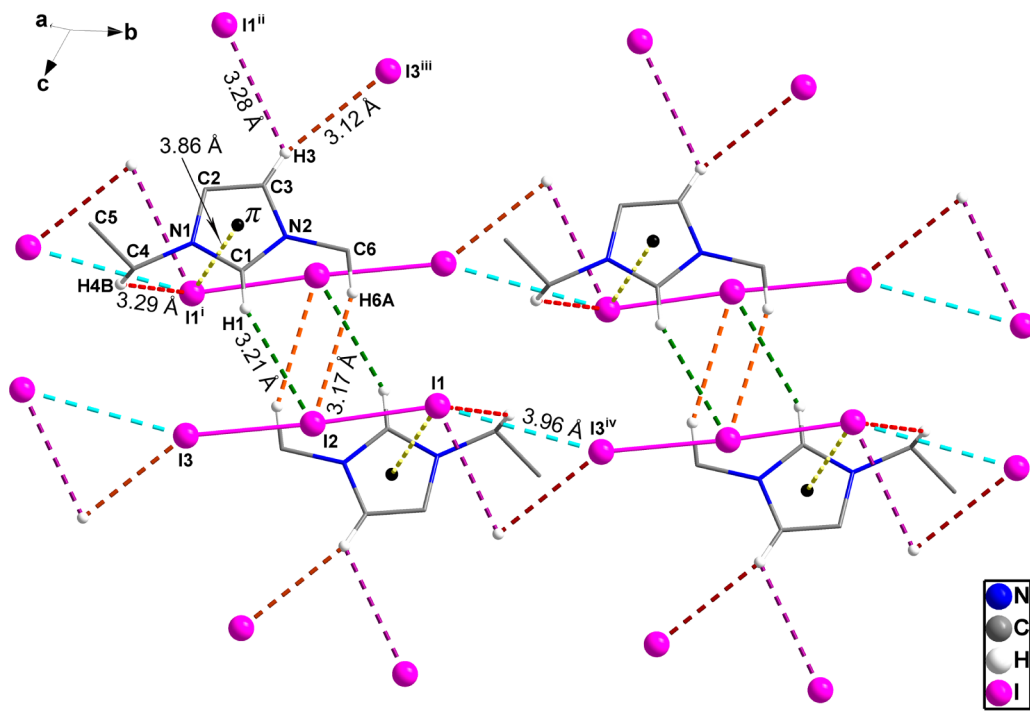


Figure 6. Packing network in $[\text{emim}][\text{I}_3]$ showing the C–H \cdots I hydrogen bonding interactions. Symmetry codes: (i) $1 - x, 1 - y, 1 - z$; (ii) $x, -1 + y, -1 + z$; (iii) $x, y, -1 + z$; (iv) $x, 1 + y, z$.

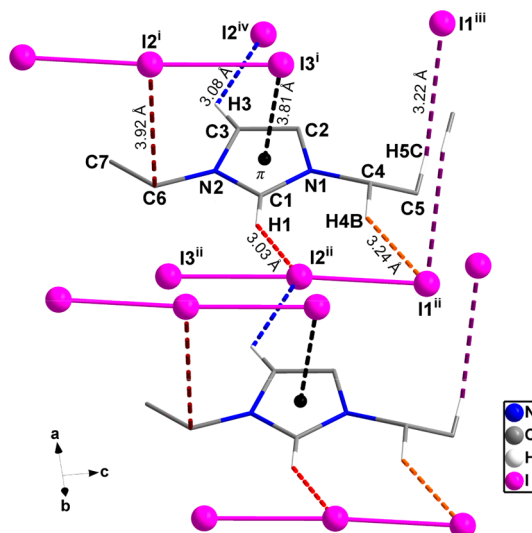


Figure 7. Packing in the network of the $[veim][I_3]$ crystal showing the C–H···I hydrogen bonding and I– π interactions. Symmetry codes: (i) $1+x, y, z$; (ii) $-x, 1-y, -z$; (iii) $1+x, y, 1+z$; (iv) $-x, -y, -z$.

crystal one of the terminal iodine atoms is not involved in hydrogen bonding, and there are no I···I interactions between the anions. The imidazolium ring forms weak I– π interactions with the anion ($I_3^{\cdot\cdot\cdot}\pi = 3.81 \text{ \AA}$). Both hydrogen bonding and π interactions are extremely common in imidazolium-based ionic liquids and have been studied in detail.^{34,56–58}

In an effort to crystallize higher polyiodide species, $[dmim]I$ ($dmim =$ the 1,3-dimethylimidazolium),^{59,60} a solid at room temperature, was reacted with I_2 in molar ratios ranging from 1:1 to 1:5. Crystals amenable to X-ray diffraction analysis were obtained from the 1:3 system containing the higher polyiodide $[I_7]^-$ anion.

The asymmetric unit of $[dmim][I_7]$ (Figure 8, left) contains two types of symmetrical $[I_7]^-$ anion structures each differing only slightly. Each $[I_7]^-$ anion is composed of a symmetrical linear $[I_3]$ subunit and two $[I_2]$ subunits, and, hence, the structure can be described as $[I_3]^- \cdot 2[I_2]$ type.⁶¹ The I–I distances in the $[I-I-I]$ subunits ($I1-I2 = 2.9196(10)$ and $I3-I4 = 2.9276(9) \text{ \AA}$) are typical of symmetrical $[I_3]^-$ anions.² The

I–I distances in the $[I_2]$ subunits ($I5-I6 = 2.7416(11)$ and $I7-I8 = 2.7367(11) \text{ \AA}$) are close in value to that found in elemental iodine.⁵⁵ The $[I-I-I]$ subunits interact with the $[I_2]$ subunits via weak I···I bonds ($I2-I7 = 3.228$ ($I2-I7$) and $I4-I5 = 3.214 \text{ \AA}$), forming a Z-type $[I_7]^-$ structure (Figure 8, right). The building block of the Z-type $[I_7]^-$ anion interacts with other anions via weak I···I bonds forming extended zigzag 3-dimensional structures with the I···I distances ranging from 4.02 to 4.29 \AA (Figure 9).

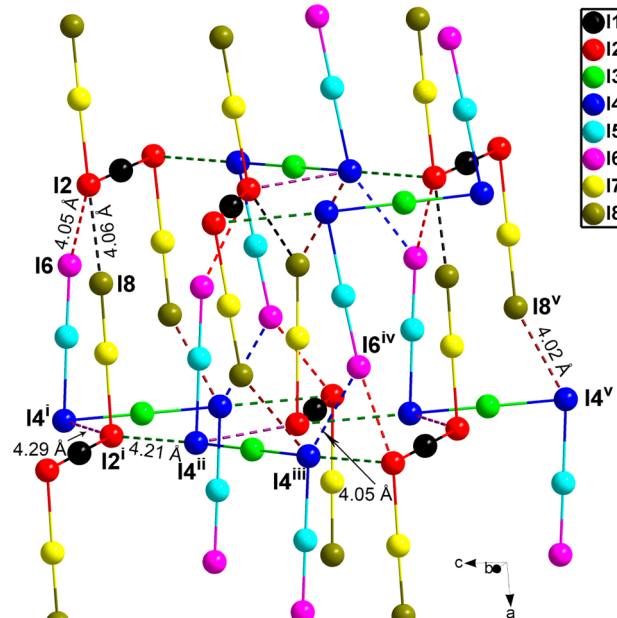


Figure 9. Packing of the $[I_7]^-$ anion showing the I···I interactions. Symmetry codes: (i) $1+x, y, 1+z$; (ii) $1+x, 1/2-y, 1/2+z$; (iii) $1-x, 1/2+y, 1/2-z$; (iv) $1-x, 1-y, -z$; (v) $1-x, -y, -z$.

Inspection of the crystal packing in $[dmim][I_7]$ reveals that the cations are distributed in channels inside a polyiodide network, that is, a “channel inclusion feature,”⁴³ encasing an imidazolium cation (Figure 10). The spacefill view shows that the cavities are filled by the cations forming a compact

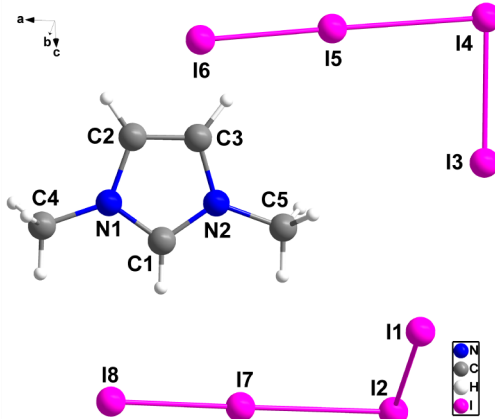


Figure 8. ORTEP representation of the structure of $[dmim][I_7]$ (left) and the two symmetrical $[I_7]^-$ anion structures created by symmetry operation (right). Selected bond lengths (\AA) and angles (deg): N(1)–C(1) 1.345(12), N(2)–C(1) 1.341(12), C(2)–C(3) 1.34(3), I(1)–I(2) 2.9196(10), I(3)–I(4) 2.9276(9), I(5)–I(6) 2.7416(11), I(7)–I(8) 2.7367(11), N(2)–C(1)–N(1) 109.8(10), I(2)–I(1)–I(2A)^{#1} 180.0, I(4)–I(3)–I(4A) 180.0.

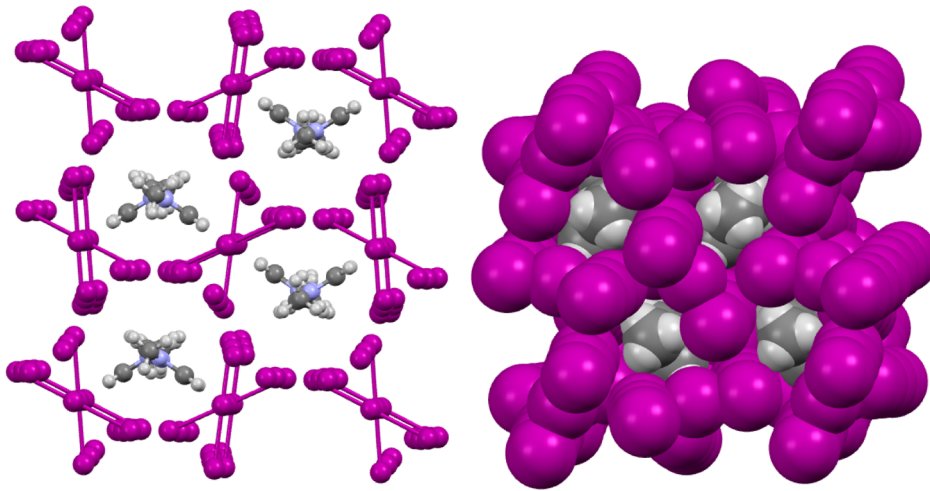


Figure 10. Packing in $[dmim][I_7]$ showing the cations distributed in channels surrounded by the anionic polyiodide network (left) and a spacefill view of the packing (right).

Table 1. Crystal Data and Structure Refinement for [emim][I₃], [vmim][I₃], and [dmim][I₇]

compound	[Emim][I ₃]	[Vmim][I ₃]	[Dmim][I ₇]
chemical formula	C ₆ H ₁₁ I ₃ N ₂	C ₇ H ₁₁ I ₃ N ₂	C ₅ H ₉ I ₇ N ₂
FW (g mol ⁻¹)	491.87	503.88	985.44
temperature (K)	100(2)	100(2)	140(2)
wavelength (Å)	0.71073	0.71073	0.71073
crystal system	triclinic	triclinic	orthorhombic
space group	P $\bar{1}$	P $\bar{1}$	Pbc a
unit cell dimensions			
<i>a</i> (Å)	7.7818(8)	7.3285(14)	18.508(4)
<i>b</i> (Å)	9.6471(6)	9.6040(13)	14.610(3)
<i>c</i> (Å)	9.7496(8)	9.831(4)	13.627(3)
α (deg)	117.253(4)	99.57(2)	90
β (deg)	91.954(7)	100.46(2)	90
γ (deg)	107.325(6)	98.957(17)	90
<i>V</i> (Å ³)	608.49(9) Å ³	658.5(3)	3684.8(13)
<i>Z</i>	2	2	8
<i>D</i> _{calcd} (g cm ⁻³)	2.685	2.541	3.553
μ (mm ⁻¹)	7.660	7.081	11.770
<i>F</i> (000)	440	452	3392
crystal size (mm ³)	0.47 × 0.44 × 0.25	0.405 × 0.270 × 0.212	0.36 × 0.28 × 0.25
Θ range for data collection (deg)	3.04 to 27.50	3.364 to 27.490	2.32 to 30.01
index ranges			
<i>h</i>	-10/10	-9/9	-25/26
<i>k</i>	-12/12	-12/12	-19/19
<i>l</i>	-12/12	-12/12	-19/19
measd. reflns.	9205	14021	9919
independent reflns	2776 [<i>R</i> (int) = 0.0225]	3021 [<i>R</i> (int) = 0.0440]	5234 [<i>R</i> (int) = 0.0455]
completeness (%)	99.10	99.50	97.30
absorption correction	semiempirical from equivalents	semiempirical from equivalents	semiempirical from equivalents
max. and min transmission	0.7456 and 0.4242	1.0000 and 0.4261	0.30 and 0.20
refinement method	full-matrix least-squares on <i>F</i> ²	full-matrix least-squares on <i>F</i> ²	full-matrix least-squares on <i>F</i> ²
data/restraints/parameters	2776/0/103	3021/0/111	5234/0/133
GOF ²	1.212	1.182	1.155
<i>R</i> 1 ^a [<i>I</i> > 2σ(<i>I</i>)]	0.0203	0.0783	0.0775
<i>wR</i> 2 ^b	0.0440	0.2278	0.2101
<i>R</i> 1 ^a (all data)	0.0239	0.0892	0.0913
<i>wR</i> 2 ^b	0.0451	0.2379	0.2556
largest diff. peak and hole (Å ⁻³)	0.683 and -0.720 e	5.163 and -1.330 e	3.356 and -4.788 e

^a $R_1 = \sum |F_o| - |F_c| / \sum |F_o|$, $wR_2 = \{\sum [w(F_o^2 - F_c^2)^2] / \sum [w(F_o^2)^2]\}^{1/2}$. ^bGOF = $\{\sum [w(F_o^2 - F_c^2)^2] / n - p\}^{1/2}$ where *n* is the number of data and *p* is the number of parameters refined.

structure. From the NMR spectroscopic studies it is not unreasonable to assume that similar motifs, albeit less rigid, exist in [pmim][I]/I₂ systems and related mixtures. In DSSCs and iodination reactions elemental iodine is often applied in large excess (up to a 5 molar ratio),^{15,16} where the polyiodide anions shield the hydrogen atoms in the cation and, simultaneously, weaken and polarize the I—I bond, facilitating a Grotthuss bond-exchange process^{23,24} and accounting for the high conductivity in [pmim][I]/I₂ mixtures^{23,24} and enhanced reactivities in iodination reactions.²¹

CONCLUDING REMARKS

Ionic liquids, typically based on imidazolium cations, doped with I₂ have a wide and diverse range of applications. Herein, we studied the systematic addition of I₂ to different imidazolium-based ionic liquids by NMR spectroscopy showing that the extent of shielding of the protons of the imidazolium cation increases with the size of the polyiodide anion generated. Several polyiodide salts were studied in the solid state revealing extensive C—H···I—I—I and π···I—I interactions that rationalize the changes observed in the NMR spectra of the cations. Overall, these interactions lengthen, polarize, and apparently weaken the I—I bonds. These features are consistent with the significant increase in the conductivity of polyiodide systems and the high reactivity of I₂-doped (polyiodide) ionic liquids in iodination reactions.

EXPERIMENTAL SECTION

The ionic liquids [pmim]I, [bmim]I, [bmim][PF₆][−], and [Emim][BF₄][−] were purchased from Iolitec AG, Germany, and [pmim][Tf₂N][−]⁶², [pmim]Br,⁴⁴ [omim]Cl,⁴² [veim]I,⁵¹ and [dmim]I⁵⁹ were prepared according to literature protocols. All ionic liquids were dried under vacuum for 3 d at 100 °C prior to use. Elemental iodine was purchased from Aldrich.

¹H, ¹³C and ¹⁹F NMR Spectroscopic Studies. All ¹H (400.13 MHz) and ¹³C (100.62 MHz) NMR spectra were recorded on a Bruker Avance II 400 spectrometer at 298 K using a sealed C₆D₆ capillary for locking. The ¹⁹F NMR spectra were recorded using capillary sealed with D₂O saturated with NaBF₄. Typically, the ionic liquid (ca. 0.5 mL) was introduced into a dry 5 mm NMR tube placed in a Schlenk tube under nitrogen at room temperature. The required amount of elemental iodine was added. The resulting mixture was ultrasonicated for 3 min prior to analysis.

Structure Determination in the Solid State. Single crystals of [emim][I₃], [veim][I₃], and [dmim][I₇] were obtained by slowly cooling the liquid from 60 to −20 °C over a period of 24 h. Diffraction data (except [dmim][I₇]) were measured at low temperature [100(2) K] using Mo Kα radiation on a Bruker APEX II CCD diffractometer equipped with a κ-geometry goniometer. The data sets were reduced by EvalCCD⁶³ and then corrected for absorption.⁶⁴ The data collection of [dmim][I₇] was collected at low temperature [140(2) K] using Mo Kα radiation on a mar345dtb system in combination with a Genix Hi-Flux small focus generator (*maruX* system). Data reduction was performed using *automar*.⁶⁵ The solutions and refinements were performed with *SHELX*.⁶⁶ The crystal structures were refined using full-matrix least-squares based on F² with all non-hydrogen atoms anisotropically defined. Hydrogen atoms were placed in calculated positions by means of the riding model. Details of crystal data and structure refinement for [emim][I₃], [vmim][I₃], and [dmim][I₇] are provided in Table 1.

ASSOCIATED CONTENT

Supporting Information

The Supporting Information is available free of charge on the ACS Publications website at DOI: [10.1021/acs.inorgchem.5b02021](https://doi.org/10.1021/acs.inorgchem.5b02021). CCDC reference numbers 1429051, 1429051,

and 1429052 contain the supplementary crystallographic data for the X-ray studies reported in this paper. These data can be obtained free of charge at www.ccdc.cam.ac.uk/conts/retrieving.html or from the Cambridge Crystallographic Data Centre, e-mail: deposit@ccdc.cam.ac.uk

X-ray crystallographic data, including illustrated structures. (CIF)

NMR spectra with illustrated molecular structures. (PDF)

AUTHOR INFORMATION

Corresponding Author

*Phone: +41-21-6939854. Fax: +41-21-6939853. E-mail: paul.dyson@epfl.ch.

Notes

The authors declare no competing financial interest.

ACKNOWLEDGMENTS

We thank the EPFL and Swiss National Science Foundation for financial support. We thank Prof. D.-R. Zhu (NanJing Tech Univ.) for valuable discussions and Dr. E. Solari (EPFL) for the assistance with the crystal structure determinations.

REFERENCES

- Blake, A. J.; Devillanova, F. A.; Gould, R. O.; Li, W. S.; Lippolis, V.; Parsons, S.; Radek, C.; Schroder, M. *Chem. Soc. Rev.* **1998**, 27, 195–205.
- Svensson, P. H.; Kloo, L. *Chem. Rev.* **2003**, 103, 1649–1684.
- Tebbe, K. F.; Buchem, R. *Angew. Chem., Int. Ed. Engl.* **1997**, 36, 1345–1346.
- Svensson, P. H.; Raud, G.; Kloo, L. *Eur. J. Inorg. Chem.* **2000**, 2000, 1275–1282.
- Svensson, P. H.; Bengtsson-Kloo, L.; Persson, P. *J. Chem. Soc., Dalton Trans.* **1998**, 1425–1429.
- Tebbe, K. F.; Gilles, T. Z. *Anorg. Allg. Chem.* **1996**, 622, 138–148.
- Chow, H.; Dean, P. A. W.; Craig, D. C.; Lucas, N. T.; Scudder, M. L.; Dance, I. G. *New J. Chem.* **2003**, 27, 704–713.
- Garcia, M. D.; Marti-Rujas, J.; Metrangolo, P.; Peinador, C.; Pilati, T.; Resnati, G.; Terraneo, G.; Ursini, M. *CrystEngComm* **2011**, 13, 4411–4416.
- Paulsson, H.; Berggrund, M.; Fischer, A.; Kloo, L. *Eur. J. Inorg. Chem.* **2003**, 2003, 2352–2355.
- Owens, B. B.; Patel, B. K.; Skarstad, P. M.; Warburton, D. L. *Solid State Ionics* **1983**, 9–10, 1241–1245.
- Licht, S.; Khaselev, O.; Ramakrishnan, P. A.; Faiman, D.; Katz, E. A.; Shames, A.; Goren, S. *Sol. Energy Mater. Sol. Cells* **1998**, 51, 9–19.
- Yourey, W.; Weinstein, L.; Amatucci, G. G. *Solid State Ionics* **2011**, 204, 80–86.
- Rajpure, K. Y.; Bhosale, C. H. *Mater. Chem. Phys.* **2000**, 63, 263–269.
- Owens, B. B.; Bottelberghe, J. R. *Solid State Ionics* **1993**, 62, 243–249.
- Hagfeldt, A.; Boschloo, G.; Sun, L. C.; Kloo, L.; Pettersson, H. *Chem. Rev.* **2010**, 110, 6595–6663.
- Wu, J. H.; Lan, Z.; Lin, J. M.; Huang, M. L.; Huang, Y. F.; Fan, L. Q.; Luo, G. G. *Chem. Rev.* **2015**, 115, 2136–2173.
- Chiappe, C.; Pieraccini, D. *Arkivoc* **2002**, 249–255.
- Ren, Y. M.; Cai, C. *Synth. Commun.* **2010**, 40, 1670–1676.
- Ren, Y. M.; Cai, C. *Tetrahedron Lett.* **2008**, 49, 7110–7112.
- Liu, C. F.; Zhang, A. P.; Li, W. Y.; Yue, F. X.; Sun, R. C. *Ind. Crops Prod.* **2010**, 31, 363–369.
- Dewan, M.; Kumar, A.; Saxena, A.; De, A.; Mozumdar, S. *Tetrahedron Lett.* **2010**, 51, 6108–6110.
- Yan, C. Y.; Mu, T. C. *Phys. Chem. Chem. Phys.* **2014**, 16, 5071–5075.

- (23) Jerman, I.; Jovanovski, V.; Vuk, A. S.; Hocevar, S. B.; Gaberscek, M.; Jesih, A.; Orel, B. *Electrochim. Acta* **2008**, *53*, 2281–2288.
- (24) Thorsmolle, V. K.; Rothenberger, G.; Topgaard, D.; Brauer, J. C.; Kuang, D. B.; Zakeeruddin, S. M.; Lindman, B.; Gratzel, M.; Moser, J. E. *ChemPhysChem* **2011**, *12*, 145–149.
- (25) Miao, J. L.; Hu, C. H.; Chen, H. Y.; Yuan, G. Z.; Nie, Y. *Acta Crystallogr., Sect. E: Struct. Rep. Online* **2009**, *65*, O1780.
- (26) Groessl, M.; Fei, Z. F.; Dyson, P. J.; Katsyuba, S. A.; Vikse, K. L.; McIndoe, J. S. *Inorg. Chem.* **2011**, *50*, 9728–9733.
- (27) Blackburn, G. M.; Lockwood, G.; Solan, V. *J. Chem. Soc., Perkin Trans. 2* **1976**, 1452–1456.
- (28) Bonhote, P.; Dias, A. P.; Papageorgiou, N.; Kalyanasundaram, K.; Gratzel, M. *Inorg. Chem.* **1996**, *35*, 1168–1178.
- (29) McGuinness, D. S.; Mueller, W.; Wasserscheid, P.; Cavell, K. J.; Skelton, B. W.; White, A. H.; Englert, U. *Organometallics* **2002**, *21*, 175–181.
- (30) Leadbeater, N. E.; Torenius, H. M.; Tye, H. *Tetrahedron* **2003**, *59*, 2253–2258.
- (31) Weingartner, H. *Curr. Opin. Colloid Interface Sci.* **2013**, *18*, 183–189.
- (32) Suarez, P. A. Z.; Einloft, S.; Dullius, J. E. L.; de Souza, R. F.; Dupont, J. *J. Chim. Phys. Phys.-Chim. Biol.* **1998**, *95*, 1626–1639.
- (33) Giernoth, R.; Bankmann, D.; Schlorer, N. *Green Chem.* **2005**, *7*, 279–282.
- (34) Katsyuba, S. A.; Griaanova, T. P.; Vidis, A.; Dyson, P. J. *J. Phys. Chem. B* **2009**, *113*, 5046–5051.
- (35) Marincola, F. C.; Piras, C.; Russina, O.; Gontrani, L.; Saba, G.; Lai, A. *ChemPhysChem* **2012**, *13*, 1339–1346.
- (36) Cha, S.; Ao, M.; Sung, W.; Moon, B.; Ahlstrom, B.; Johansson, P.; Ouchi, Y.; Kim, D. *Phys. Chem. Chem. Phys.* **2014**, *16*, 9591–9601.
- (37) Remsing, R. C.; Liu, Z. W.; Sergeyev, I.; Moyna, G. *J. Phys. Chem. B* **2008**, *112*, 7363–7369.
- (38) Hesse-Ertelt, S.; Heinze, T.; Kosan, B.; Schwtkal, K.; Meister, F. Solvent Effects on the NMR Chemical Shifts of Imidazolium-Based Ionic Liquids and Cellulose Therein. In *Utilization of Lignocellulosic Materials*; Heinze, T., Janura, M., Koschella, A., Eds. Wiley: Weinheim, Germany, 2010; Vol. 294-II, pp 75–89.
- (39) Zhao, Y.; Gao, S. J.; Wang, J. J.; Tang, J. M. *J. Phys. Chem. B* **2008**, *112*, 2031–2039.
- (40) Remsing, R. C.; Wildin, J. L.; Rapp, A. L.; Moyna, G. *J. Phys. Chem. B* **2007**, *111*, 11619–11621.
- (41) Wulf, A.; Fumino, K.; Ludwig, R. *Angew. Chem., Int. Ed.* **2010**, *49*, 449–453.
- (42) Huddleston, J. G.; Visser, A. E.; Reichert, W. M.; Willauer, H. D.; Broker, G. A.; Rogers, R. D. *Green Chem.* **2001**, *3*, 156–164.
- (43) Herbstein, F. H.; Reisner, G. M.; Schwotzer, W. *J. Inclusion Phenom.* **1985**, *3*, 173–182.
- (44) Bohm, V. P. W.; Herrmann, W. A. *Chem. - Eur. J.* **2000**, *6*, 1017–1025.
- (45) Izgorodina, E. I.; Forsyth, M.; MacFarlane, D. R. *Aust. J. Chem.* **2007**, *60*, 15–20.
- (46) Fernandes, A. M.; Rocha, M. A. A.; Freire, M. G.; Marrucho, I. M.; Coutinho, J. A. P.; Santos, L. M. N. B. F. *J. Phys. Chem. B* **2011**, *115*, 4033–4041.
- (47) Shaplov, A. S.; Vlasov, P. S.; Armand, M.; Lozinskaya, E. I.; Ponkratov, D. O.; Malyshkina, I. A.; Vidal, F.; Okatova, O. V.; Pavlov, G. M.; Wandrey, C.; Godovikov, I. A.; Vygodskii, Y. S. *Polym. Chem.* **2011**, *2*, 2609–2618.
- (48) Kurig, H.; Vestli, M.; Tonurist, K.; Janes, A.; Lust, E. *J. Electrochem. Soc.* **2012**, *159*, A944–A951.
- (49) Tempel, D. J.; Henderson, P. B.; Brzozowski, J. R.; Pearlstein, R. M.; Cheng, H. S. *J. Am. Chem. Soc.* **2008**, *130*, 400–401.
- (50) Choudhury, A. R.; Winterton, N.; Steiner, A.; Cooper, A. I.; Johnson, K. A. *J. Am. Chem. Soc.* **2005**, *127*, 16792–16793.
- (51) Wang, Y. Q.; Sun, Y. M.; Song, B.; Xi, J. T. *Sol. Energy Mater. Sol. Cells* **2008**, *92*, 660–666.
- (52) Tebbe, K. F.; Gilles, T. Z. *Anorg. Allg. Chem.* **1996**, *622*, 1587–1593.
- (53) Wang, Y.; Xue, Y. Q.; Wang, X. P.; Cui, Z. X.; Wang, L. L. *J. Mol. Struct.* **2014**, *1074*, 231–239.
- (54) Abdulsada, A. K.; Greenway, A. M.; Hitchcock, P. B.; Mohammed, T. J.; Seddon, K. R.; Zora, J. A. *J. Chem. Soc., Chem. Commun.* **1986**, 1753–1754.
- (55) van Bolhuis, F.; Koster, P. B.; Migchelsen, T. *Acta Crystallogr.* **1967**, *23*, 90–91.
- (56) Zhao, D. B.; Fei, Z. F.; Scopelliti, R.; Dyson, P. J. *Inorg. Chem.* **2004**, *43*, 2197–2205.
- (57) Matthews, R. P.; Welton, T.; Hunt, P. A. *Phys. Chem. Chem. Phys.* **2014**, *16*, 3238–3253.
- (58) Martinez, C. R.; Iverson, B. L. *Chem. Sci.* **2012**, *3*, 2191–2201.
- (59) Chan, B. K. M.; Chang, N. H.; Grimmett, M. R. *Aust. J. Chem.* **1977**, *30*, 2005–2013.
- (60) Chen, W. Z.; Liu, F. H.; You, X. Z. *J. Solid State Chem.* **2002**, *167*, 119–125.
- (61) Poli, R.; Gordon, J. C.; Khanna, R. K.; Fanwick, P. E. *Inorg. Chem.* **1992**, *31*, 3165–3167.
- (62) Mazille, F.; Fei, Z. F.; Kuang, D. B.; Zhao, D. B.; Zakeeruddin, S. M.; Gratzel, M.; Dyson, P. J. *Inorg. Chem.* **2006**, *45*, 1585–1590.
- (63) Duisenberg, A. J. M.; Kroon-Batenburg, L. M. J.; Schreurs, A. M. M. *J. Appl. Crystallogr.* **2003**, *36*, 220–229.
- (64) Blessing, R. H. *Acta Crystallogr., Sect. A: Found. Crystallogr.* **1995**, *51*, 33–38.
- (65) Automar, release 2.8.0; Marresearch GmbH: Germany 2011.
- (66) Sheldrick, G. M. *Acta Crystallogr., Sect. A: Found. Crystallogr.* **2008**, *64*, 112–122.